

POD ANALYSIS OF THE REACTION RATES IN A TURBINE STAGE WITH IN SITU COMBUSTION

Sterian DANAILA, Dragos ISVORANU, Constantin LEVENTIU

University Politehnica of Bucharest, Romania

DOI: 10.19062/1842-9238.2015.13.3.14

Abstract: This paper presents the in-situ combustion concept and preliminary numerical results in a one stage turbine combustor. The main purpose of the simulation is to assess the stability of the in situ combustion with respect to the unsteadiness induced by the rotor-stator interaction. In order to identify information on the sources of instability for this complex flow, proper orthogonal decomposition technique is adopted to analyze the natural patterns and couplings between various modes of pressure, temperature, velocity and chemical production rate distributions. The major find of this investigation is that contrary to all other primitive variables, the reconstruction of chemical reaction rates needs a larger number of energy modes to attain a reasonable normalized error.

Keywords: turbine in-situ combustion; POD reconstruction;

1. INTRODUCTION

Turbine combustion is a relatively recent concept, and the amount of work published in the open literature is presently quite limited. A turbine-combustor is defined as a turbine in which fuel is injected and burned. The process of combustion in the turbine is called *in situ* reheat.

A review of recent work carried out in the field is concentrated on four related areas [1]: (i) thermodynamic cycle analysis, (ii) reacting mixing layers in accelerating flows, (iii) flame holding in high speed flows and (iv) compact combustors.

A comparison of the Brayton, regenerative Brayton, Ericsson, Carnot, and Isothermal expansion, isentropic compression cycles, concludes that the Ericsson cycle has the highest thermal efficiency and highest dimensionless net work; therefore it should be the prime candidate for GTE cycle [2].

A second option is the isothermal expansion, isentropic compression cycle whose thermal efficiency and net work are better than those of the Brayton and regenerative Brayton cycles.

Thermodynamic cycle analysis has been carried out for both continuous combustion [3] and for inter-stage combustion [4], using component efficiencies based on typical, real-life values.

These studies demonstrate performance gains related to lower fuel consumption, higher specific thrust, and enhanced operational speed and compressor pressure ratios for both turbojet and turbofan engines. In addition, a CFD analysis based on the RANS equations coupled with a two-step, global, finite rate model for methane combustion [5] showed for a land-based GTE a power increase of up to 5.1% in a four-stage turbine combustor with a 2% mass flow rate of fuel [6]. The results are clearly showing benefits of the technology.

2. CFD COMPUTATIONAL MODEL

The computational model is based on a CAD model inspired from a true one row turbine with 26 stator vanes and 61 rotor blades that expands 8.1 kg/s burnt gas from 911 kPa total pressure and 1263 K total temperature.

The rotation speed of the rotor wheel is 22000 RPM. Apart from previous attempts, the salient feature of this CFD approach is the new fuel injection concept consisting in a perforated pipe placed at mid-pitch in the stator row passage.

The flow and combustion are modelled by the Reynolds averaged Navier-Stokes equations coupled with the species transport equations. The turbulence model used is the scale adaptive simulation-shear stress trans-
port.

The chemistry turbulence interaction is described in terms of finite rate-eddy dissipation concept. The choice we have taken was to increase the inlet total temperature at 1550 K in order to succeed in firing up the flow of injected pure methane using the two-step, global, finite rate chemical mechanism of Westbrook and Dryer [7]. This increase amounts to the modern combustors usual outlet temperature.

The simulation was performed in ANSYS CFX simulation environment. The composition of the inlet burnt gas is given in terms of the mass fraction distribution computed from equilibrium calculations at the given inlet temperature: $Y_{\text{CO}_2} = 0.064$, $Y_{\text{CO}} = 10^{-6}$, $Y_{\text{O}_2} = 0.0152$, $Y_{\text{H}_2\text{O}} = 0.035$, $Y_{\text{N}_2} = 0.751$.

The fuel inlet parameters are: 50 m/s, 350 K and 0.00127 kg/s.

The turbulence intensity for both inlets was 5%. The ignition of the cold, slow fuel jet diffused in the hot, fast stream of oxidizer is delayed until the mixture achieves both the necessary local oxidizer-fuel ratio and the temperature to boost the chemical mechanism.

The enhanced turbulence in the wake of the stator airfoil trailing edge accelerates the mixing between the two streams.

The flame front starts just before entering the rotor and moves downstream. The flame is broken into patches of burning mixture by the intermittent passage of the rotor leading edges.

The patches of burning mixture slide along the rotor airfoil, continuing to burn due to the lower velocities in the boundary layer. These patches of burning mixture expand their volume due to the temperature raise and pressure drop. Coherent flame structures are formed downstream of rotor's trailing edge.

The rotor-stator interaction unsteadiness effect can be expressed in terms of the outlet average temperature variation which amounts to 10-15 degrees K for the *in situ* reheat.

3. POD METHODOLOGY. MODAL DECOMPOSITION

The Proper Orthogonal Decomposition (POD) is a method that reconstructs a set of data from its projection on an optimal basis.

Besides using an optimal basis for reconstructing data, POD does not use any prior knowledge of the data set. Because of this POD is also used in natural patterns analysis of the flow field.

To rebuild the dynamic behavior of a system, POD breaks down data into two parts: a time dependent part, that generates the amplitude coefficients $a_k(t)$ and a spatial coordinates dependent part that yields a orthonormal functional basis $\psi_k(\mathbf{x})$. The reconstructed model reads:

$$u(\mathbf{x}, t) = \sum_{k=1}^M a_k(t) \cdot \psi_k(\mathbf{x}) \quad (1)$$

where M is the number of data snapshots. The reconstruction dataset error is:

$$\varepsilon(\mathbf{x}, t) = u(\mathbf{x}, t) - \sum_{k=1}^M a_k(t) \cdot \psi_k(\mathbf{x}) \quad (2)$$

The functional basis on which this set is reconstructed is optimal because the average of the squared error is minimized for any number $m \leq M$ of base functions from all possible sets of orthogonal functions $\varepsilon_m = \langle\langle \varepsilon, \varepsilon \rangle\rangle$. In reference [8] was showed that the minimization condition is equivalent to maximizing the ratio:

$$\lambda = \langle\langle (u, \psi) \rangle\rangle / (\psi, \psi) \quad (3)$$

which happens when the base functions $\psi_k(\mathbf{x})$ are solutions of the Fredholm integral equation:

$$\sum_{j=1}^M \int R_{ij}(\mathbf{x}, \mathbf{x}') \cdot \psi_j(\mathbf{x}') d\mathbf{x}' = \lambda \psi_i(\mathbf{x}) \quad (4)$$

where R_{ij} is the correlation kernel.

Following this approach, one transforms the decomposition into an eigenvalue problem where λ_k is the associated eigenvalue to the eigenmode ψ_k .

As the inner product (\cdot, \cdot) can be thought of in terms of "energy", the value of λ_k is linked to the energy content of the ψ_k characteristic.

Hence, for short, the POD optimization process represents the way in which the dataset is projected on a basis that maximizes the energy content. The first mode will be the most energetic.

In the field of fluid mechanics, two main approaches have been used: the first one, the classical, continuous POD was promoted by Lumley [8]; the second one is based on the so called snapshot approach and originates in the works of Sirovitch [9]. The main difference between these approaches is the way in which the correlation matrix is built.

Following the Sirovitch methodology, we will build the time-correlation matrix:

$$C = \iint u(\mathbf{x}, t)u(\mathbf{x}, t')d\Omega \quad (5)$$

which is only of the order of the square of time snapshots. The spatial proper modes are to be computed from:

$$\psi_k(\mathbf{x}) = \frac{1}{\sqrt{\lambda_k}} \int \phi_k(t)u(\mathbf{x}, t)dt \quad (6)$$

where ϕ_k are the eigenvectors corresponding to λ_k .

3. DISCRETE POD-SNAPSHOT FORMULATION

We start from a set of M snapshots obtained from the numerical simulation of the given model. The simulation can be performed either with a commercial or in-house code. The sampling rate must comply with Nyquist-Shannon [10] criterion used for signal reconstruction. The construction of the correlation matrix is done as follows, either for a vector valued or scalar valued function. Assuming that the quantity of interest is denoted by u , first we have to arrange all its values for a certain snapshot in a vector with dimension N (N could be very large depending on the discretized model). Then, for each following snapshot, we proceed identically in order to build the next $N \times M$ matrix. The correlation matrix is then built as

$$C_{M \times M} = W_C^T \cdot W_C \cdot$$

The previous square matrix is positive definite, hence it yields positive,

$$W_C = \begin{bmatrix} u(\mathbf{x}_1, t_1) & u(\mathbf{x}_1, t_2) & \cdots & u(\mathbf{x}_1, t_M) \\ u(\mathbf{x}_2, t_1) & u(\mathbf{x}_2, t_2) & \cdots & u(\mathbf{x}_2, t_M) \\ \vdots & \vdots & \cdots & \vdots \\ u(\mathbf{x}_N, t_1) & u(\mathbf{x}_N, t_2) & \cdots & u(\mathbf{x}_N, t_M) \end{bmatrix} \quad (7)$$

real eigenvalues λ_k and the associated eigenvectors ϕ_k that are rearranged in a matrix Φ from the most energetic to the least energetic content (eigenvalues in decreasing order). The eigenmodes with only spatial dependence ψ_k are obtained as:

$$\Psi_{N \times M} = (W_{N \times M} \cdot \Phi_{M \times M}) \cdot L_{M \times M} \quad (8)$$

where $L_{M \times M}$ is a diagonal square matrix with elements $1/\sqrt{\lambda_k}$ arranged in descending order. The reconstruction of $\tilde{u}(\mathbf{x}, t)$ based on $m < M$ modes follows the equation:

$$\tilde{u}(\mathbf{x}, t) = \sum_{k=1}^m \sqrt{\lambda_k} \phi_k(t) \psi_k(\mathbf{x}) = \sum_{k=1}^m a_k(t) \psi_k(\mathbf{x}) \quad (9)$$

Considering the flow variables of interest, ROM models (Eq. 9) can be devised for each one of them.

Another approach takes into account a different structure for the inner product defined in Eq. (5). For example, following Rowley et al. [11], one can consider

$$(\mathbf{q}_1, \mathbf{q}_2) = \int_{\Omega} (\rho_1 \rho_2 + u_1 u_2 + v_1 v_2 + w_1 w_2 + p_1 p_2) d\Omega \quad (10)$$

but in this case, care should be taken to use an appropriate non-dimensional form. The discrete counterpart of Eq. (10) can be deduced from Eq. (7) by simply putting one quantity below the other in the vectors chosen for the matrix construction.

4. RESULTS

The simulation performed for the turbine combustor offered the requested snapshots with a sampling rate of 10 snapshots per cycle. Herein, a cycle is defined as the time requested for the rotor to travel a distance equal to the stator pitch length at midspan. First 41 out of 200 snapshots were analyzed. The configuration space contains density, absolute pressure, velocity components in stationary frame, temperature, static entropy, Mach number and the reaction rates for methane and carbon mono-oxide oxidation. Applying the procedures described by Eqs. (7)-(9) we obtained the specific eigenspectra. Figure (1) illustrates these spectra CO and methane decomposition reactions, while Fig. (2) shows the almost harmonic behavior of temporal coefficients for CH4 reaction rate.

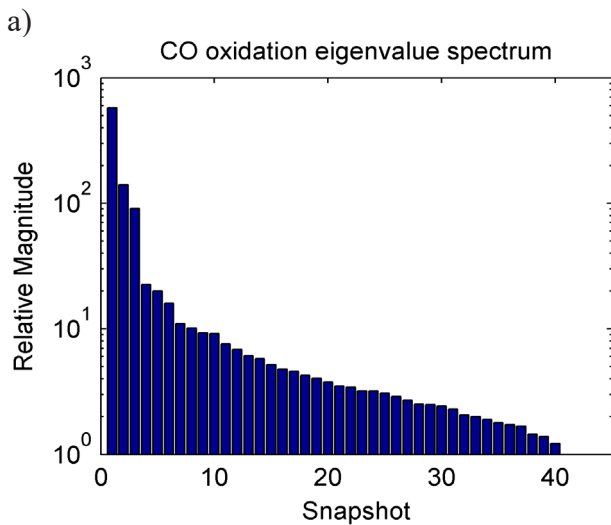
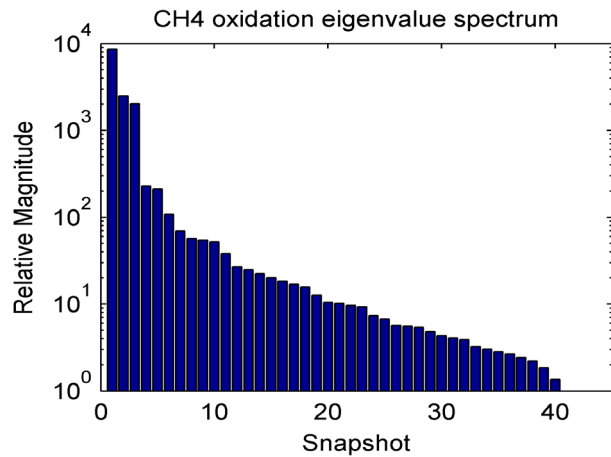


Fig. 1 Eigenspectrum for the reactions of the chemical mechanism.

The most outstanding feature of the eigenspectra for the specified configuration space is the similarity of the eigenvalue modal distributions among all flow variables except for the two reaction rates. The “energy” spectrum for the methane oxidation rate needs at least 20 modes to cover 95% of the total energy content, while for the rest of the variables 1 mode is sufficient.

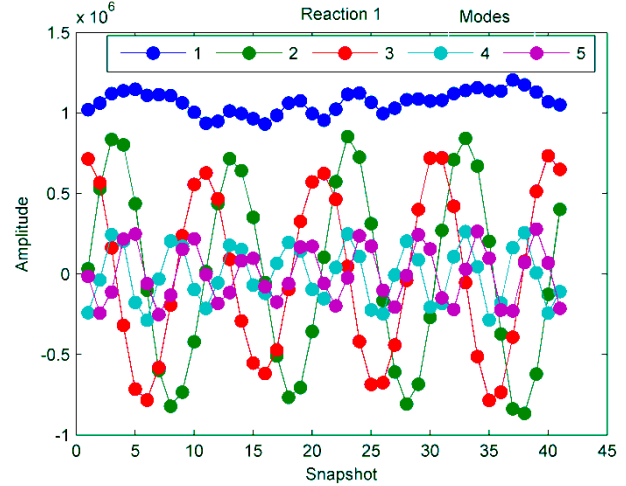


Fig. 2 Amplitude variation for the first five modes for methane decomposition.

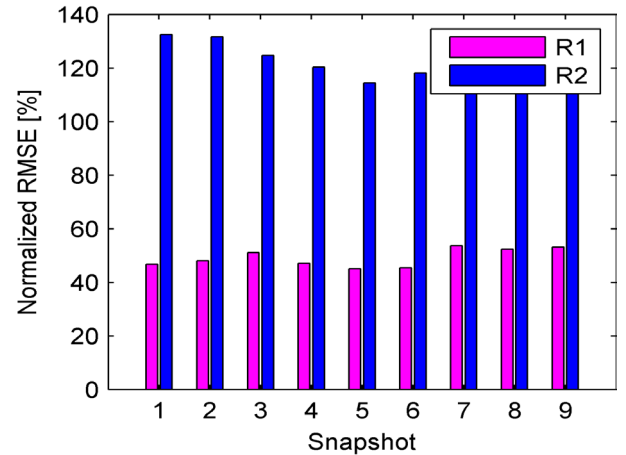
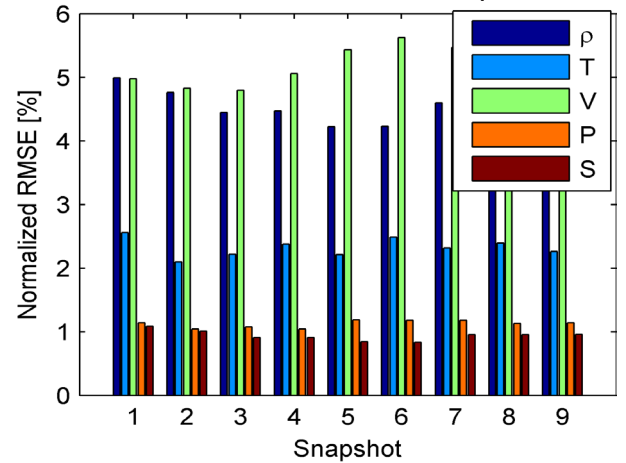


Fig. 3 Five modes reconstruction accuracy

Five modes are needed for CO oxidation rate. The same observation becomes apparent from the normalized RMSE of the reconstructed snapshots displayed in Fig. 3.

The error is unacceptable for CH₄ oxidation rate and still too large for CO oxidation rate. The natural patterns of the reactive flow are associated with the eigenmodes ψ_k distributions.

As expected, the reaction rates and temperature modes are well coupled up until the third mode (Fig. 4) even if the nodes and antinodes switch places along the rotor-stator interface. Beyond third mode, these correlations are lost for CH₄ reaction rate but remain visible for CO reaction rate and temperature up to fifth mode.

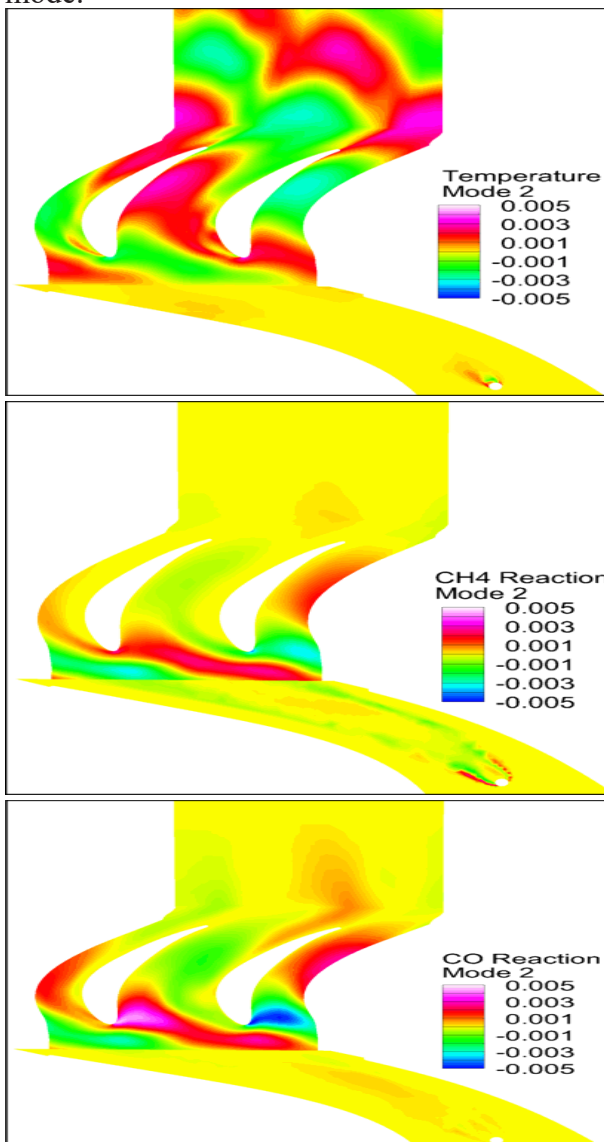


Fig. 4 Temperature and reaction rates correlations on the second mode.

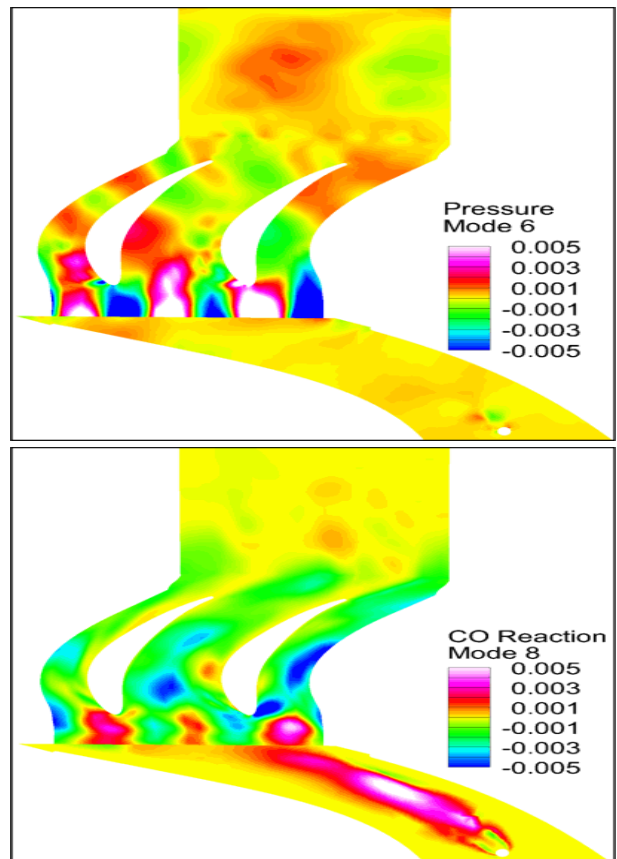


Fig. 5 Acoustic correlations between pressure and CO reaction rate.

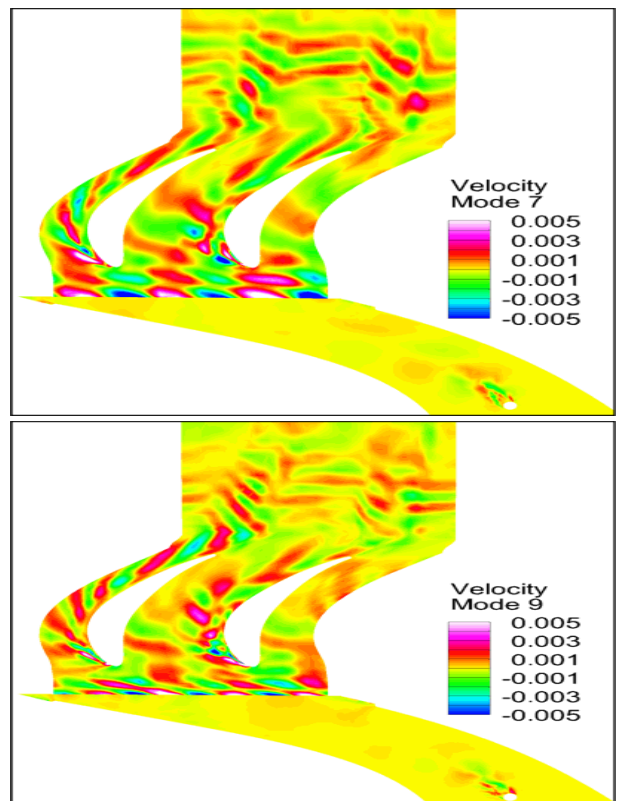


Fig. 6. Velocity odd-even decoupling in the wake of the injection pipe.

The next acoustic modes bring new correlations between absolute pressure and CO reaction rate along the rotor-stator interface which are apparent from Fig. 5.

Odd-even decoupling and oscillations are characteristics emerging from higher acoustic modes for pressure and velocity, especially in the wake of the injection pipe, as depicted in Figs. 5a-5b and Fig. 6.

CONCLUSIONS

In this study we have emphasized the possibility of using POD technique in order to obtain information on the natural patterns for various thermodynamic and flow quantities defining the process of gas expansion in a turbine burner. The precision of the reconstruction depends on how many eigenvectors (basis functions) are considered. The analysis shows only the first step in obtaining an useful reduced order model. The salient features observed concern especially the reaction rates described in the Westbrook-Dryer mechanism. It seems that higher modes for CH₄ oxidation need to be taken into account which amounts to either using smaller time steps in the numerical simulation approach or revisit the reaction mechanism and find appropriate reaction rate coefficients. Due to the large errors in the reconstruction of the reaction rates snapshots, a reduced order model is not feasible based on the available CFD data. The stability, sensitivity or inverse analyses have to be postponed until solving the previous mentioned shortcomings resulted from the POD investigation.

ACKNOWLEDGMENT

This research was funded by the by the Joint Applied Research Project PN-II-PT-PCCA-2013-4, with the support of ANCS, CNDI – UEFISCDI, project no. 286/2014.

BIBLIOGRAPHY

1. W.A. Sirignano, D. Dunn-Rankin, F. Liu, B. Colcord, S. Puranam, "Turbine Burners: Flameholding in Accelerating Flow", *AIAA Journal*, Vol. 50, No. 8, (2012).
2. W.H. Krase, "Ericsson Cycle Gas Turbine Powerplants", *Technical Report Rand Corporation*, R-2327-DOE, (1979).
3. Simpson, J. R. and G. C. May. Reheat apparatus for a gas turbine engine. Unites States Patent Office: 3,141,298, Rolls-Royce Limited, Derby, England, (1964).
4. Althaus, R., F. Farkas, P. Graf, F. Hausermann, and E. Kreis. Method of operating gas turbine group with reheat combustor. Unites States Patent Office: 5,454,220, Asea-Brown-Boveri, Baden, Switzerland, (1995)
5. D. D. Isvoranu, P. G. A. Cizmas, "Numerical simulation of Combustion and Rotor-Stator Interaction in a Turbine Combustor," *International Journal of Rotating Machinery*, **9**, 363-374, (2003).
6. S. Chambers, H. Flitan, P. Cizmas, D. Bachovchin, T. Lippert, D. Little, "The Influence of In Situ Reheat on Turbine-Combustor Performance," *Journal of Engineering for Gas Turbines and Power*, **128**, 560-572, (2006).
7. C. K. Westbrook and F. L. Dryer. Simplified reaction mechanisms for the oxidation of hydrocarbon fuels in flames, *Combustion Science and Technology*, **27** 31–43, (1981).
8. Lumley, J.. *Stochastic Tools in Turbulence*. Academic Press. 1970.
9. Sirovich, L. *Turbulence and the dynamics of coherent structures*, parts I–III. *Q. Appl. Math.* **XLV** (3), (1987).
10. Jerri, A.J., The Shannon sampling theorem — Its various extensions and applications: A tutorial review, *Proceedings of the IEEE*, Volume 65, Issue 11, pp:1565 – 1596, (1977).
11. C.W., Rowley, T. Colonius and R.M. Murray, Model reduction for compressible flows using POD and Galerkin projection, *Physica D* **189** 115–129, (2004).